

# Chapter 5

## Chaos in the driven pendulum

Having studied the appearance of chaos in the logistic map, we now move on to look at how chaos arises in Hamiltonian systems.

So far the Hamiltonian systems that we have considered have had one degree of freedom and have also been conservative: the energy has been a constant of the motion. Together these two facts mean that the systems have been *integrable*. Basically, this means that there are as many conserved quantities as there are degrees of freedom. Integrable systems do not display chaotic behaviour.

So in order to study chaos in a Hamiltonian system, we either need to move to a system with two degrees of freedom, or introduce time-dependence into the Hamiltonian for a system with one degree of freedom. The second route is somewhat simpler: we can introduce a time-dependent potential that means energy is no longer conserved.

The particular example we will consider is the *vertically driven pendulum*. By controlling that amplitude of the driving we can influence the chaotic behaviour, leaving all other parameters fixed.

### 5.1 Hamiltonian for the driven pendulum

We consider a pendulum with a pivot that is driven vertically by a function  $\gamma(t)$ . The coordinates of the system are

$$x = a \sin \phi, \quad y = -a \cos \phi - \gamma(t), \quad (5.1)$$

where  $a$  is the length of the pendulum. Thus the kinetic energy is

$$T = \frac{m}{2}(\dot{x}^2 + \dot{y}^2) = \frac{m}{2}(a^2\dot{\phi}^2 - 2a\dot{\gamma}\dot{\phi}\sin\phi), \quad (5.2)$$

and the potential energy is

$$V = mgy = -mga \cos \phi - mg\gamma, \quad (5.3)$$

and is a function of time. Thus the Lagrangian is

$$\mathcal{L} = T - V = \frac{m}{2}a^2\dot{\phi}^2 - ma\dot{\gamma}\phi \sin \phi + mga \cos \phi + h(t), \quad (5.4)$$

where  $h(t) = m\dot{\gamma}^2 + mg\gamma$  is a function of time only, and hence is ignorable. (It is easy to show that it does not contribute to the equations of motion.)

The momentum conjugate to  $\phi$  for this Lagrangian is

$$p = \frac{\partial \mathcal{L}}{\partial \dot{\phi}} = m(a^2\dot{\phi} - a\dot{\gamma} \sin \phi), \quad (5.5)$$

which leads to the Hamiltonian

$$H(\phi, p, t) = \frac{(p + ma\dot{\gamma} \sin \phi)^2}{2ma^2} - mga \cos \phi. \quad (5.6)$$

However, a more convenient Hamiltonian can be obtained by making use of the property that two Lagrangians related by

$$\bar{\mathcal{L}}(q, \dot{q}, t) = \mathcal{L}(q, \dot{q}, t) + \frac{d}{dt}f(q, t) \quad (5.7)$$

describe the same motion. If we add

$$-ma \frac{d}{dt}(\dot{\gamma} \cos \phi) = -ma\ddot{\gamma} \cos \phi + ma\dot{\gamma}\dot{\phi} \sin \phi \quad (5.8)$$

to Eq. (5.4) we get a new Lagrangian

$$\mathcal{L} = T - V = \frac{m}{2}a^2\dot{\phi}^2 + ma(g - \ddot{\gamma}) \cos \phi, \quad (5.9)$$

which shows that vertical acceleration has the same effect as a time-varying gravitational field. The conjugate momentum is now the angular momentum

$$\ell = \frac{\partial \bar{\mathcal{L}}}{\partial \dot{\phi}} = ma^2\dot{\phi} = J\dot{\phi}, \quad (5.10)$$

where  $J = ma^2$  is the moment of inertia of the pendulum. The Hamiltonian is

$$\bar{H}(\phi, \ell, t) = \frac{\ell^2}{2J} - J\omega_0^2 \left(1 - \frac{\ddot{\gamma}}{g}\right) \cos \phi, \quad (5.11)$$

where  $\omega_0^2 = g/a$ .

## 5.2 Equations of motion

Hamilton's equations for the system are

$$\dot{\phi} = \frac{\partial \bar{H}}{\partial \ell} = \frac{\ell}{J}, \quad \dot{\ell} = -\frac{\partial \bar{H}}{\partial \phi} = -J\omega_0^2 \sin \phi \left(1 - \frac{\ddot{\gamma}}{g}\right), \quad (5.12)$$

which can be combined to give a single second-order differential equation

$$\ddot{\phi} = -\omega_0^2 \sin \phi \left( 1 - \frac{\ddot{\gamma}}{g} \right). \quad (5.13)$$

We now assume a periodic driving function

$$\gamma t = \gamma_0 \cos(\omega_D t) \quad \Rightarrow \quad \ddot{\gamma} = -\gamma_0 \omega_D^2 \cos(\omega_D t), \quad (5.14)$$

where  $\omega_D$  is the driving frequency and  $\gamma_0$  is the amplitude of the driving. By introducing the dimensionless parameters

$$\kappa = \left( \frac{\omega_0}{\omega_D} \right)^2, \quad \epsilon = \omega_D^2 \frac{\gamma_0}{g} = \frac{\gamma_0 \omega_0^2}{g \kappa}, \quad \tau = \omega_D t, \quad (5.15)$$

the equation of motion for the driven pendulum becomes

$$\ddot{\phi} = -\kappa \sin \phi (1 - \epsilon \cos \tau). \quad (5.16)$$

We now look at methods to study systems such as this.

### 5.3 Poincarè sections

The phase portraits for non-autonomous Hamiltonian systems such as described by Eq. (5.16) can get extremely messy, as the trajectories are no longer curves with constant energy. This is demonstrated in Fig. 5.1 Instead, it can be very useful to plot points in phase space that represent the system at a discrete moment in time. We replace the continuous curve with points that represent  $(\varphi, \ell)$  as specific moments in time separated by  $\Delta\tau$

The trajectory on the left in Fig. 5.1 had a period  $T = 2\pi/\omega(H)$ . If we choose  $\Delta\tau = T/4$  then only four points will appear. Likewise, if we choose  $\Delta\tau = T/16$  then only sixteen points will appear. This is illustrated in Fig. 5.2

In general, if  $\Delta\tau = \frac{m}{n}T$ , where  $m, n$  are positive integers, then there will be at most  $n$  possible distinct points in phase space. However: If  $\Delta\tau = \alpha T$ , where  $\alpha$  is any *irrational* number, then in the limit that  $\tau \rightarrow \infty$  an infinite number of points will build up giving a solid line.

The Poincarè section can be viewed as subjecting the continuous trajectory in phase space to a *strobe* of frequency  $\Omega = 2\pi/\Delta\tau$ . We have

$$\frac{\Delta\tau}{T} = \frac{2\pi/\Omega}{2\pi/\omega(H)} = \frac{\omega(H)}{\Omega}. \quad (5.17)$$

If this is irrational: an infinite number of points will appear. Otherwise, there will be a finite number of points

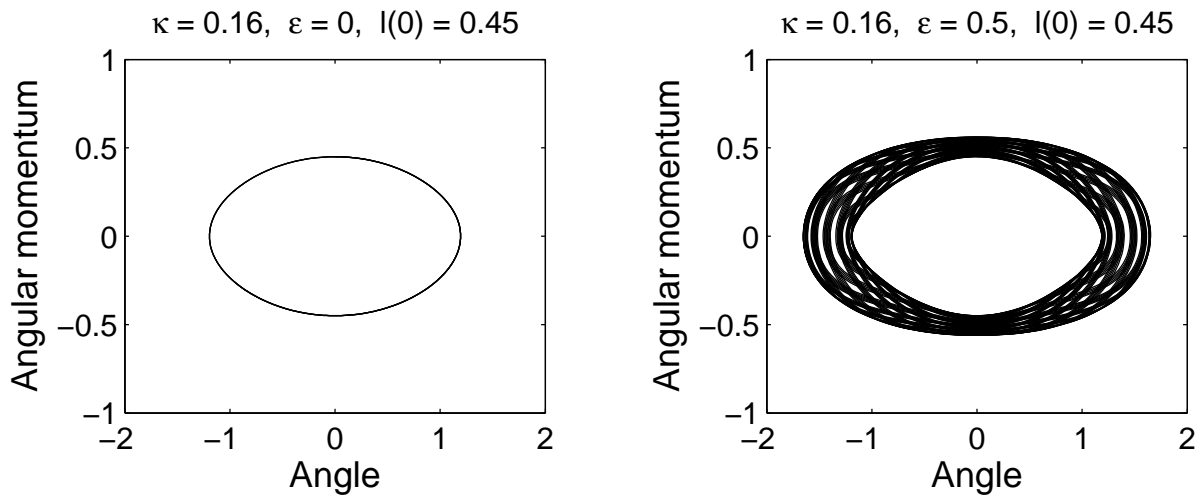


Figure 5.1: Phase portrait for a single trajectory of the pendulum: undriven (left) and driven (right).

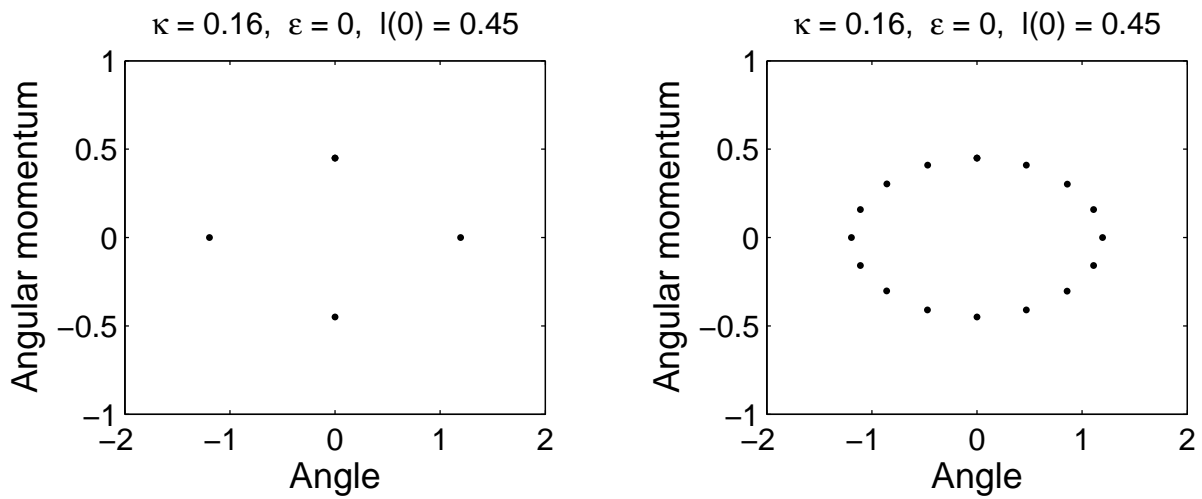


Figure 5.2: Example of Poincaré sections: left  $\Delta\tau = T/4$ , right  $\Delta\tau = T/16$ .

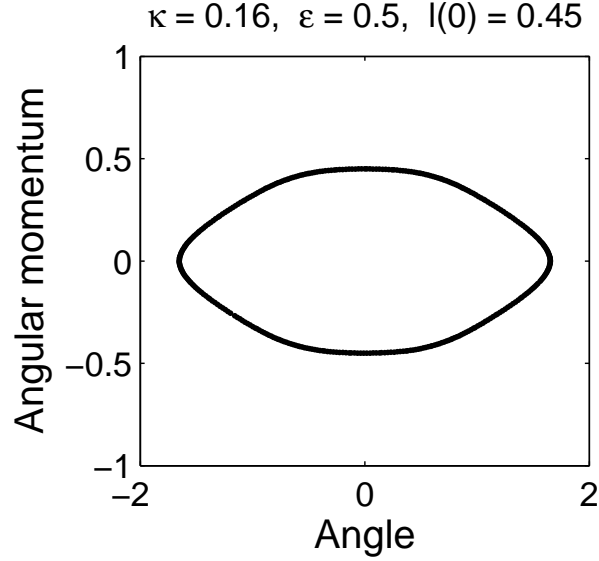


Figure 5.3: Poincaré section for the same parameters as the trajectory on the right of Fig. 5.1, sampled at the driving frequency  $\omega_D$  for 350 driving periods. This is a sufficient number of points to pretty much fill in the entire curve.

Poincaré sections are a very useful concept in the analysis of complicated systems, and we use it for the driven pendulum. It is a graphical representation of the mapping of the point  $(q_n, p_n)$  at time  $\tau = n\Delta\tau$  to the point  $(q_{n+1}, p_{n+1})$ , where we have  $q_n = q(n\Delta\tau)$ ,  $n = 0, 1, 2, \dots$ , etc. This can also be written

$$(q_{n+1}, p_{n+1}) = T(q_n, p_n) \quad (5.18)$$

for an appropriate operator  $T$ , in a similar manner to the 1D maps that we looked at earlier. However, in this situation it is very hard or impossible to find a closed expression for  $T$ .

In Poincaré sections for driven systems we typically sample the system once every driving period i.e.  $\Omega = \omega_D$ .

## 5.4 Irrational Poincaré sections

We take the parameters  $l(0) = 2/3$ ,  $\kappa = 0.16$ , and show what happens as the strength of the driving  $\epsilon$  is increased. For these parameters we have  $\omega_D/\omega(H) = 3.15853287332306$  which is close to being irrational (MATLAB shows that  $10420/3299 = 3.15853288875417$  gets the first seven decimal places correct). Hence, the Poincaré section forms a closed curve for  $\epsilon = 0$ , as is shown in Fig. 5.4.

Note that the curves *remain closed* as  $\epsilon$  increases. However: this suddenly breaks down above a certain  $\epsilon$  and the motion becomes chaotic.

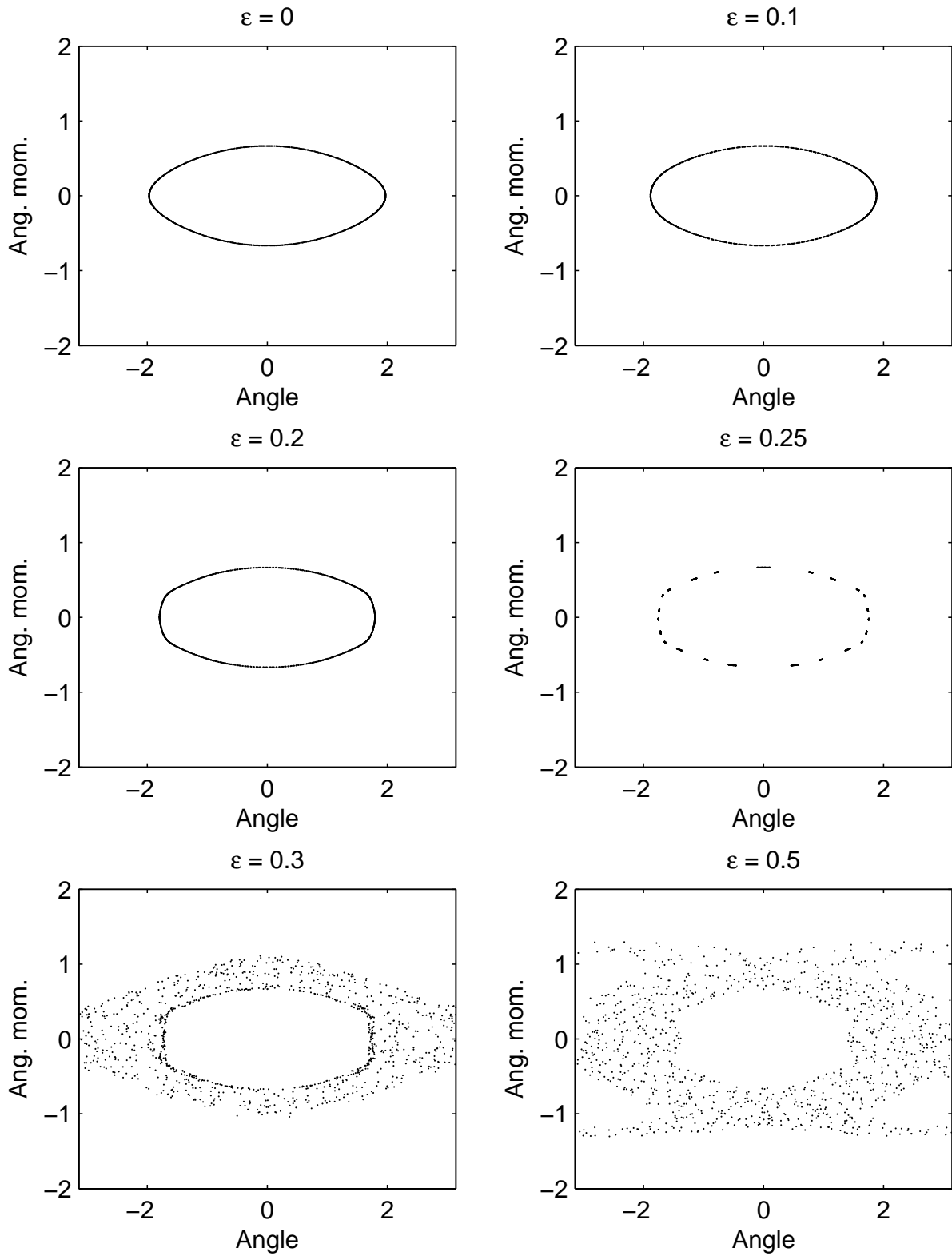


Figure 5.4: Poincaré section for  $\ell(0) = 2/3, \phi(0) = 0, \kappa = 0.16$  and a range of drive strengths  $\epsilon$  as indicated.

This is an important concept in dynamics: if  $\omega(H)/\omega_D$  is irrational then for a sufficiently small drive the Poincarè section remains a closed curve but is distorted.

**KAM theorem (Kolmogorov, Arnold and Moser):** “For sufficiently irrational surfaces and sufficiently weak perturbations, the surfaces of constant action are preserved under the perturbation and are not destroyed.”

This theorem has broad scope: it does not refer to specific trajectories or time scales. It defines a type of global stability.

## 5.5 Rational Poincarè sections

Here we take the initial parameters  $\ell(0) = 0.58517059, \kappa = 0.16$  which have been chosen such that  $\omega_D/\omega(H) = 3$ . Hence for the undriven system with  $\epsilon = 0$  we get three points only, as is shown in Fig. 5.5.

However, as soon as  $\epsilon > 0$  the points become an island chain. This is certainly not a mere distortion. This is an example of a resonance, and is a typical feature of such systems. They play a crucial role in the transition to chaotic dynamics. Within the islands there still exist what are known as fixed points. However, eventually these break up as well when  $\epsilon$  continues to get larger.

## 5.6 Transition to chaos

Finally we finish this section by giving an example of a global Poincarè section changes as we increase the driving frequency.

Poincarè sections were generated by solving Hamilton’s equations numerically for 500 driving periods, with a range of initial conditions with  $\phi(0) = 0$  and  $\ell(0)$  equally spaced from -3 to 3, with  $\omega_D = 0.8\omega_0, \kappa = 1.5625$ .

The unperturbed Poincarè section ( $\epsilon = 0$ ) looks very similar to our previous phase portrait for the pendulum.

As  $\epsilon$  is increased, chaotic layers first appear near the separatrices. This is typical behaviour for such systems.

An important feature is that new islands of stability appear in the region of the rational Poincarè surfaces. As  $\epsilon$  increases, the area of the chaotic region grows and secondary islands appear.

You will get a chance to investigate this in the computer lab.

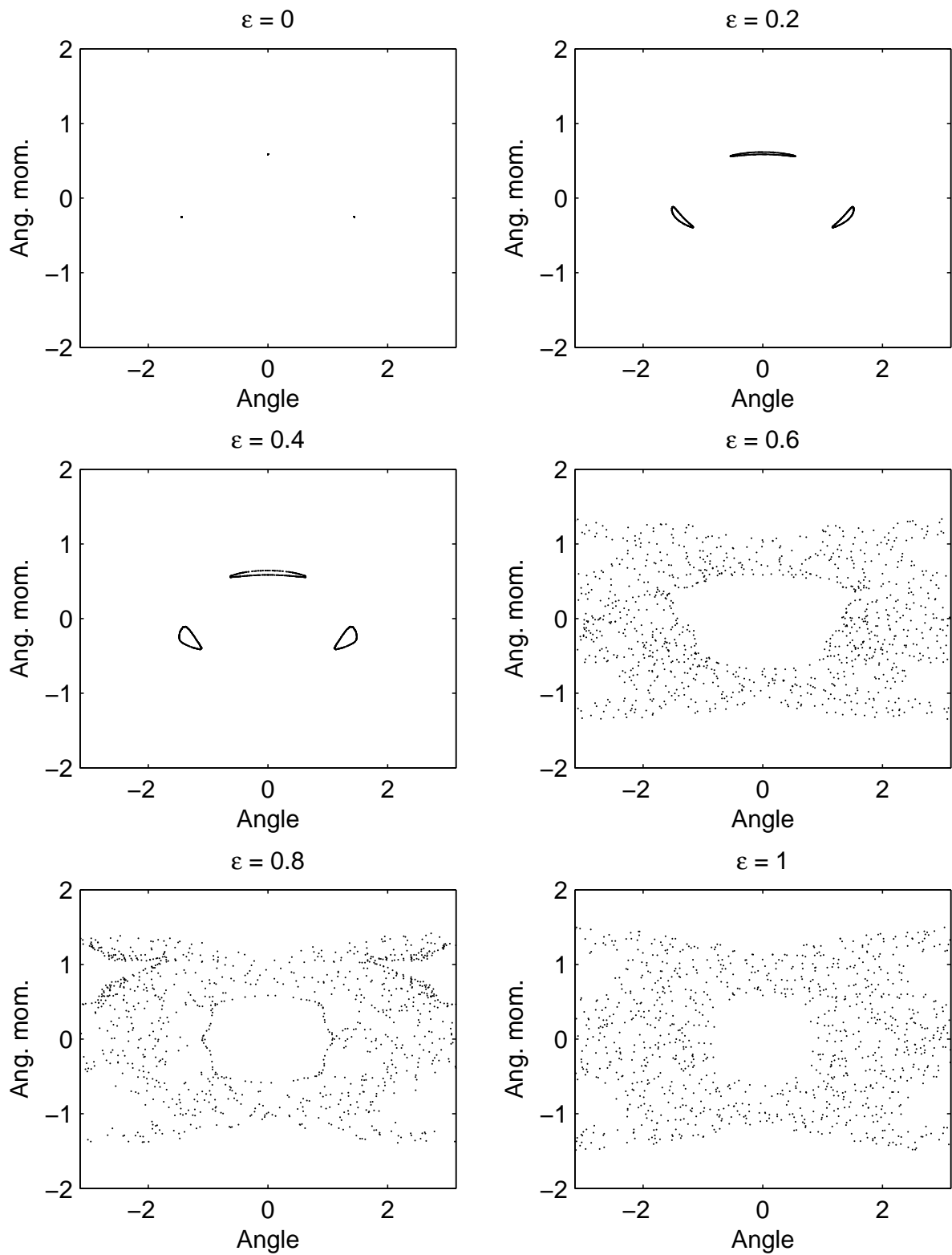


Figure 5.5: Poincaré section for  $\ell(0) = 0.58517059, \phi(0) = 0, \kappa = 0.16$  and a range of drive strengths  $\epsilon$  as indicated.



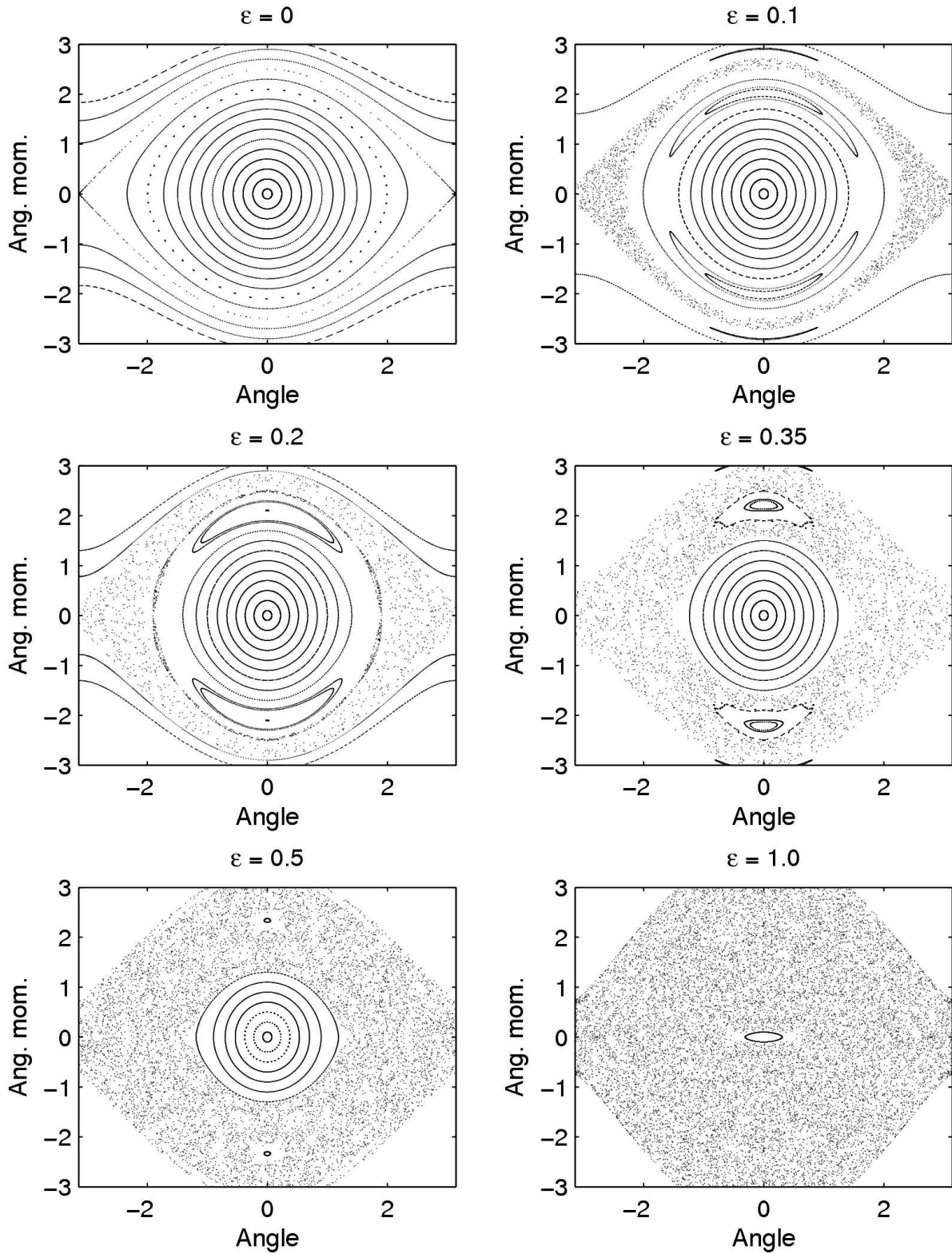


Figure 5.6: Poincaré sections for  $\omega_D = 0.8\omega_0$ ,  $\kappa = 1.5625$ . The islands that appear on the top and bottom contain period-one fixed points. The chaos layer increases as  $\epsilon$  is increased, and will eventually engulf the entire phase space.

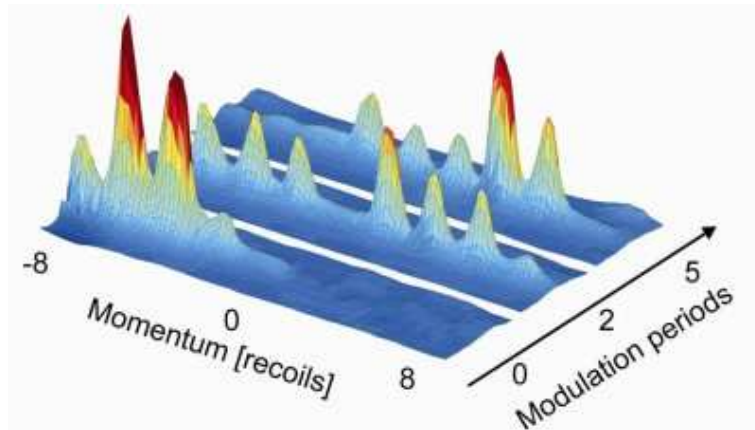


Figure 5.7: Dynamical tunnelling. At a particular point in time most of the atoms have a negative momentum, however at a later time at the same point in the drive period the atoms have mostly positive momentum. Classically this behaviour cannot occur.

## 5.7 Quantum dynamical tunneling (for interest only)

The driven potential for the pendulum can be realised for ultra-cold atoms using an intensity modulated standing wave of light.

It turns out that a classical barrier exists between trajectories located on the period-one fixed points in the Poincarè section.

However, quantum mechanically atoms localised on one island can tunnel through to the opposite island — this is known as “*dynamical tunnelling*”.

While this was first predicted in 1981, it was finally observed by UQ researchers with a Bose-Einstein condensate in collaboration with Nobel prize winner Bill Phillips in 2001: W. Hensinger *et al.*, Nature **412**, 52 (2001).

Follow-up experiments and theory still happening at UQ.